Vibrational Analysis of Amino Acids and Short Peptides in Hydrated Media. IV. Amino Acids with Hydrophobic Side Chains: L-Alanine, L-Valine, and L-Isoleucine

ARTICLE *in* THE JOURNAL OF PHYSICAL CHEMISTRY B · APRIL 2009

Impact Factor: 3.3 · DOI: 10.1021/jp809204d · Source: PubMed

4 AUTHORS:

Belén Hernández
Université Paris 13 Nord
39 PUBLICATIONS **375** CITATIONS
SEE PROFILE

Fernando Pfluger
Université Paris 13 Nord
23 PUBLICATIONS **330** CITATIONS
SEE PROFILE

Mama Nsangou
University of Maroua
41 PUBLICATIONS **244** CITATIONS
SEE PROFILE

Mahmoud Ghomi
Université Paris 13 Nord
112 PUBLICATIONS **1,774** CITATIONS
SEE PROFILE

THE JOURNAL OF PHYSICAL CHEMISTRY B

Article

Vibrational Analysis of Amino Acids and Short Peptides in Hydrated Media. IV. Amino Acids with Hydrophobic Side Chains: l-Alanine, l-Valine, and l-Isoleucine

Bele#n Herna#ndez, Fernando Pflu#ger, Mama Nsangou, and Mahmoud Ghomi

J. Phys. Chem. B, **2009**, 113 (10), 3169-3178• DOI: 10.1021/jp809204d • Publication Date (Web): 16 February 2009

Vibrational Analysis of Amino Acids and Short Peptides in Hydrated Media. IV. Amino Acids with Hydrophobic Side Chains: L-Alanine, L-Valine, and L-Isoleucine

Belén Hernández,[†] Fernando Pflüger,[†] Mama Nsangou,[‡] and Mahmoud Ghomi*[,†]

Laboratoire de Biophysique Moléculaire, Cellulaire et Tissulaire (BioMoCeTi), UMR CNRS 7033, UFR SMBH, Université Paris 13, 74 rue Marcel Cachin, 93017 Bobigny cedex, France, and Département de Physique, Faculté des Sciences, Université de Ngaoundéré, BP 454, Ngaoundéré, Cameroun

Received: October 17, 2008; Revised Manuscript Received: December 04, 2008

In the framework of our investigations on the analysis of vibrational spectra of amino acids (AAs) in hydrated media, Raman scattering and Fourier transform infrared (FT-IR) attenuated transmission reflectance (ATR) spectra of three α-amino acids with hydrophobic hydrocarbon side chains, i.e., alanine, valine, and isoleucine, were measured in H_2O and D_2O solutions. The present data complete those recently published by our group on glycine and leucine. This series of observed vibrational data gave us the opportunity to analyze the vibrational features of these amino acids in hydrated media by means of the density functional theory (DFT) calculations at the B3LYP/6-31++G* level. Harmonic vibrational modes calculated after geometry optimization on the clusters containing five water molecules interacting with H-donor and H-acceptor sites of amino acids are performed and allowed the observed main Raman and infrared bands to be assigned. Additional calculations on a cluster formed by leucine (L) and five water (W) molecules and the comparison of the obtained data with those recently published by our group on L+12W, allowed us to justify the number of hydration considered in the present report.

I. Introduction

α-amino acids (α-AAs) such as alanine (A), valine (V), isoleucine (I), and leucine (L) are all formed with aliphatic side chains. For this reason, they are known as hydrophobic amino acids. This family of AAs plays an important role in protein folding[1] by creating hydrophobic pockets in soluble proteins, hardly accessible by surrounding water. They also take part in the lypophilic interactions leading to anchor membrane proteins within phospholipid bilayers[2] and in the secondary structural properties of amphiphilic and amphipathic peptides.[3−14]

Among this group of AAs, A is the structurally simplest one, with a methyl group as the side chain (Figure 1). Although it is considered as a nonessential AA, it can be found in all proteins. The other three AAs have more complex side chains, with three (in V) or four (in I and L) carbons connected to the skeletal C_α atom (Figure 1). This is the reason why these AAs are called "*branched chain*" AAs (BCAAs). BCAAs are essential in protein synthesis and are thus of a key importance in the therapy of burn victims. From a physiological point of view, BCAAs were shown to regulate the protein synthesis in skeletal muscles after exercise.[15,16]

Vibrational spectroscopy is known as a rapid and powerful tool to provide useful information on the secondary structure of peptides and proteins in aqueous solutions, through the analysis of the spectral regions named amide (I, II, III, IV,...) which are highly sensitive to the peptide backbone motions. Vibrational techniques (Raman scattering and infrared absorption) can also be used to determine molecular sites in which interactions occur between peptides or proteins and other molecules (nucleic acids, phospholipids, drugs,...). To achieve these purposes, a good knowledge of vibrational modes arising from different AAs, considered as the building blocks of peptides and proteins is necessary. Several experimental and

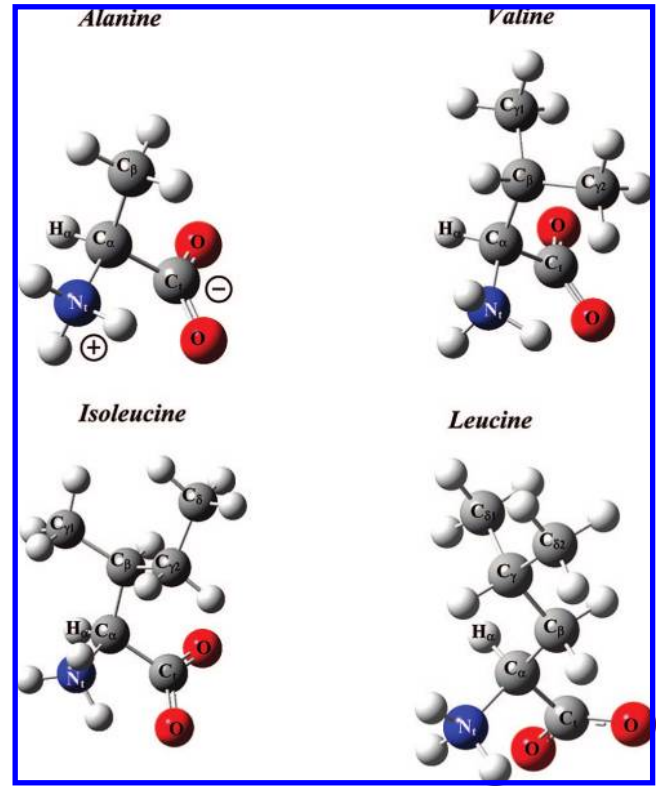

Figure 1. Branched chain amino acids (BCAAs): alanine (A), valine (V), isoleucine (I), and leucine (L). Note that all of them have hydrophobic side chains formed only by successive CH_2 and CH_3 chemical groups branched to the backbone carbon C_α.

* To whom correspondence should be addressed. E-mail: mahmoud.ghomi@univ-paris13.fr. Phone: +33-1-48388928. Fax: +33-1-48387356.
[†] Université Paris 13.
[‡] Université de Ngaoundéré.

10.1021/jp809204d CCC: $40.75
Published on Web 02/16/2009

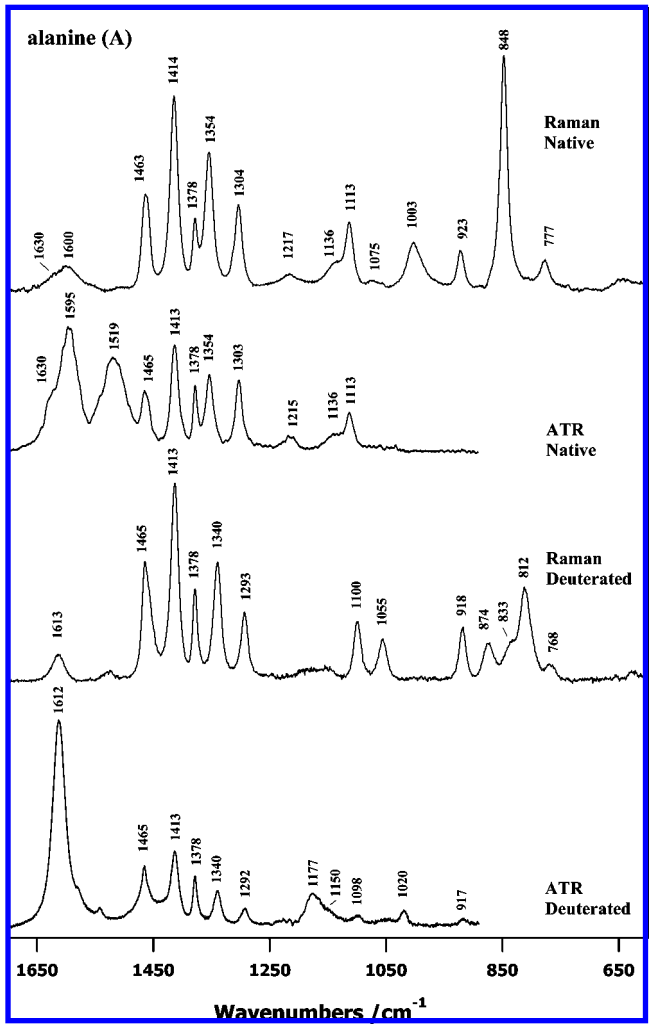

Figure 2. Vibrational spectra of alanine (A) observed in aqueous solutions. From top to bottom: Raman spectrum recorded in H_2O buffer ($\lambda_L = 488$ nm), FT-IR ATR spectrum recorded in H_2O, Raman spectrum recorded in D_2O buffer ($\lambda_L = 488$ nm), FT-IR ATR spectrum recorded in D_2O. The intensity of each observed spectrum was normalized to the most intense peak in order to facilitate their comparison.

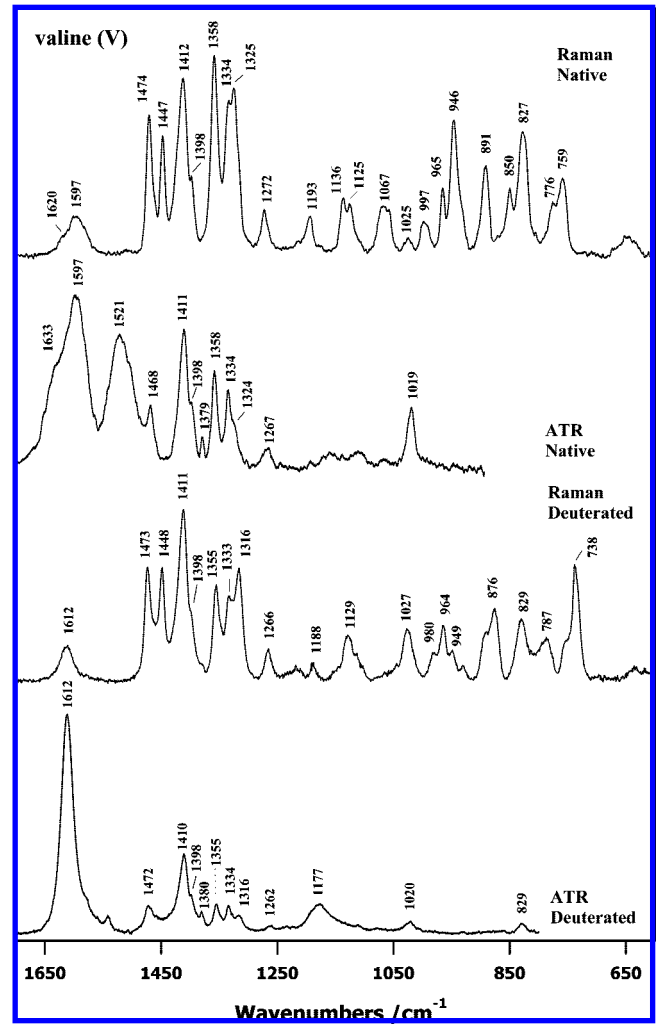

Figure 3. Vibrational spectra of valine (V) observed in aqueous solutions. From top to bottom: Raman spectrum recorded in H_2O buffer ($\lambda_L = 488$ nm), FT-IR ATR spectrum recorded in H_2O, Raman spectrum recorded in D_2O buffer ($\lambda_L = 488$ nm), FT-IR ATR spectrum recorded in D_2O. The intensity of each observed spectrum was normalized to the most intense peak in order to facilitate their comparison.

theoretical works on AAs have been reported. For instance, aqueous solution FT-IR spectra of all 20 α-AAs were reported in the 1800−500 cm^{-1} spectral region as a function of pH.[17] Attention was especially paid to the vibrational motions located below 1200 cm^{-1}. Raman spectra were discussed[18] on some AAs (including those with aliphatic side chains) and their isotopic derivatives obtained by specific deuteration on the hydrogens connected to the side chain carbons and C_α. From the theoretical point of view, the geometrical parameters of free α-alanine were studied at both Hartree−Fock (HF) and Moller−Plesset (MP2) levels of theory.[19] Density functional theory (DFT) calculations, carried out by means of B3LYP and extended basis sets, allowed confirmation of the existence of two conformers revealed by low temperature Ar matrix infrared absorption data from neutral alanine and its labile hydrogen deuterated isotopomer A-d3.[20] Theoretical calculations at the DFT/B3LYP/6-31G* level permitted the analysis of the observed vibrational absorption (VA) and vibrational circular dichroism (VCD) spectra of zwitterionic L-alanine.[21] Explicit water molecules and a dielectric medium reproducing bulk water effects have been considered in the theoretical calculations.[21] HF and DFT calculations allowed discussion and assignment of the infrared absorption spectra of alanine obtained from aqueous and solid samples as well as Raman spectra from crystal samples.[22] Among amino acids with more complex aliphatic chains, we should mention two previous reports on valine: the first one devoted to the matrix isolation infrared spectra of valine as interpreted at the DFT/B3LYP/6-31++G** level of theory[23] and the second one on the Raman spectra recorded by polarized light on the crystalline samples of valine.[24]

In manuscript I of this series,[25] we have reported the full aqueous phase vibrational analysis of two amino acids: glycine and leucine. We have also proposed a theoretical model for the solvation of these amino acids by quantum chemical calculations based on a cluster containing each amino acid and 12 surrounding water molecules mimicking the first and partially the second hydration shells in order to estimate as accurately as possible the aqueous solution geometrical and vibrational data.[25] The average number of water molecules interacting with an amino acid within its first hydration shell was discussed in several previous reports. It is now established that at least three water molecules are necessary to stabilize the zwitterionic character of an AA backbone.[26−29] From a dynamical point of view, Car−Parrinello molecular dynamics (CPMD) calculations on the intramolecular proton transfer in glycine have evidenced

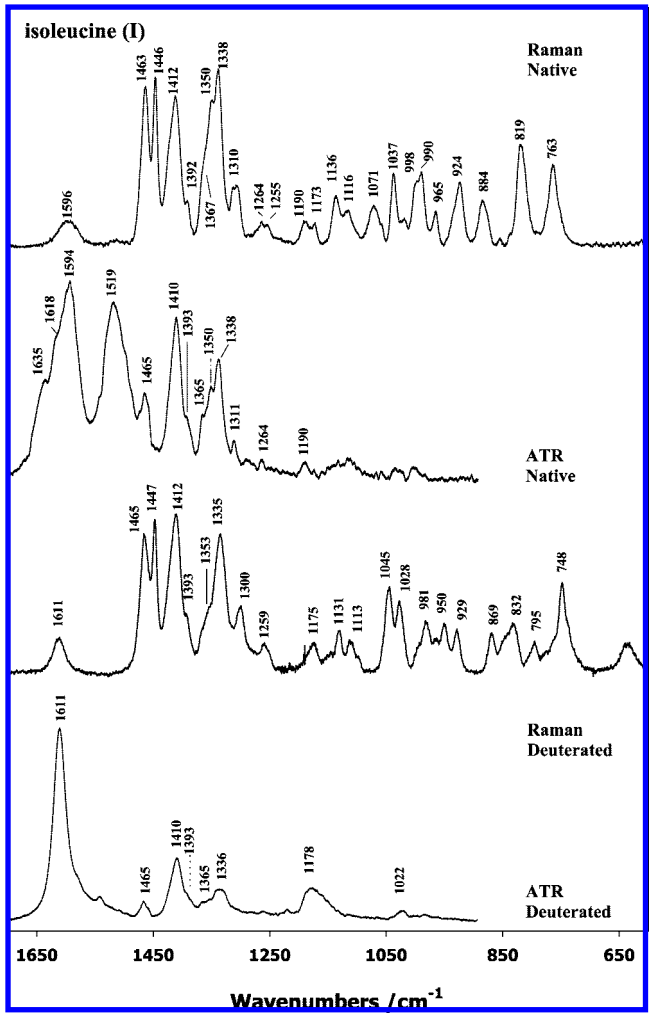

Figure 4. Vibrational spectra of isoleucine (I) observed in aqueous solutions. From top to bottom: Raman spectrum recorded in H_2O buffer ($\lambda_L = 488$ nm), FT-IR ATR spectrum recorded in H_2O, Raman spectrum recorded in D_2O buffer ($\lambda_L = 488$ nm), FT-IR ATR spectrum recorded in D_2O. The intensity of each observed spectrum was normalized to the most intense peak in order to facilitate their comparison.

that the average hydration number progresses from 5 to 8, in going from the neutral molecule to the zwitterion.[30]

In the present work, we extend our vibrational analysis to the three remaining AAs of the above-mentioned group, i.e., A, V, and I. From the experimental point of view, we present newly recorded Raman and FT-IR spectra in H_2O and D_2O. From the theoretical side, we show here our calculated results concerning the geometry and vibrational modes of hydrated amino acids at the DFT/B3LYP level, based on the clusters containing five water molecules. This number of solvent molecules is sufficient to (i) stabilize the zwitterionic character of each AA and (ii) present an adequate hydration scheme of NH_3^+ and COO^- terminals. We have justified the decrease in the number of water molecules (5 presently versus 12 in our previous calculations[25]) basically in the case of leucine through a discussion on the geometrical and vibrational data.

II. Materials and Methods

Experimental. Powder samples of the AAs were purchased from Sigma-Aldrich and used as provided. Solutions of AAs were prepared by dissolving each compound in phosphate buffer, pH (pD) = 6.8, containing 10 mM monovalent cations (Na^+ and K^+), to obtain aqueous samples of 50 mM molecular concentration used for Raman spectroscopy. FT-IR (ATR) spectra were obtained from solutions of AAs ($c = 100$ mM) directly prepared in H_2O or D_2O. Deuterated samples were prepared in D_2O (>99.8% purity, Euriso-Top CEA) under a dry air atmosphere. Room temperature Raman spectra were excited at 488 nm with an Ar^+ laser (Spectra Physics) and collected on a Jobin-Yvon T64000 spectrograph (single spectrograph configuration with a 1200 grooves/mm holographic grating and a holographic notch filter) equipped with a liquid nitrogen cooled CCD detection system (Spectrum One, Jobin-Yvon) based on a Tektronix CCD chip of 2000 × 800 pixels. The effective spectral slit width was set to ca. 5 cm^{-1}. Room temperature ATR spectra of AAs were recorded with a FT-IR Perkin-Elmer 2000 spectrophotometer equipped with an ATR accessory, under continuous dry air purge. Typically, 18 μL of sample solutions were deposited in drops on the ZnSe crystal of the ATR accessory, and spread to cover the whole surface. The infrared beam, with an effective angle of incidence of 45°, follows 12 reflections from the entrance to the exit points in the ATR crystal. Usually, 20 scans were collected with 1 cm^{-1} spectral resolution and a medium Norton Beer apodization function. Postprocessing (subtraction of buffer contribution, baseline correction, and smoothing) of Raman spectra was performed using the GRAMS/32 software (Galactic Industries). ATR data treatment was performed using the Perkin-Elmer Spectrum program and consisted only of solvent subtraction and multiple-point baseline correction. Final presentation of vibrational spectra has been performed by means of the SIGMAPLOT package.

Theoretical. As in our first paper of this series, the DFT method with B3LYP functionals was used, i.e., Becke's three-parameter (B3) exchange functional[31] along with the Lee−Yang−Parr (LYP) nonlocal correlation functional.[32] Split valence double-ζ Gaussian atomic basis sets, containing diffuse functions on both heavy and hydrogen atoms, i.e., 6-31++G*, were employed in order to account as appropriately as possible for the zwitterionic character of the amino acids in an aqueous medium. Theoretical computations have been performed on the IBM workstations using the Gaussian 03 package,[33] allowing us to achieve both molecular geometry optimization and harmonic vibration estimation. As far as the hydration number (n_w) of amino acids is concerned, we have considered a compromise between all of the previously reported calculations.[25−29] Consequently, several calculations performed on hydrated leucine (the amino acid with the largest size hydrophobic side chain) with different values of solvent molecules ($n_w < 12$) were run in order to determine the optimal number of water molecules. We have found that a cluster formed by a leucine and 5 H_2O can be finally considered as a good model for estimating the structural and vibrational data of this amino acid in hydrated medium (*vide infra*) (Figure 1). The reliability of the calculated results obtained by the value $n_w = 5$ on other AAs (A, V, and I) was also proved by further calculations. Therefore, in the present report, we only present these results (Figure 2). As in our previous calculations,[25] no additional water molecule was placed around the side chain of the AAs. In our previous calculations on hydrated uracil at the DFT/B3LYP level, we have shown in detail that basis set superposition error (BSSE) corrections are not necessary when diffuse basis sets (such as 6-31++G*) are employed.[34] No imaginary frequency was obtained in vibrational calculations, thus proving that all optimized geometries correspond well to local energy minima. Quantum mechanical results (atomic Cartesian coordinates and Cartesian force constants) were post-treated by a homemade program (BORNS) allowing removal

TABLE 1: Assignment of the Alanine (A) Vibrational Modes Observed in Aqueous Solutions[a]

alanine				alanine -deuterated			
Raman	IR	calcd	assignment(PED%)	Raman	IR	calcd	assignment (PED%)
	1630 (sh)	1764	NtH_3^+-asym bend (51)				
		1678	NtH_3^+-asym bend (45); W···NtH_3^+ (9)	1613 (m)	1612 (s)	1683	$CtOO^-$-asym st (81); Cα−Ct−O-asym bend (8)
1600 (m)	1595 (s)	1658	$CtOO^-$-asym st (54); W(H−O−H) (25)				
	1519 (s)	1603	NtH_3^+-sym bend (33); NtH_3^+ sym rock (31); W···NtH_3^+ (10)				
1463 (s)	1465 (m)	1524	Cβ-asym rock (87)	1465 (s)	1465 (m)	1524	Cβ-asym rock (88)
1414 (s)	1413 (s)	1517	Cβ-asym rock (86)	1413 (s)	1413 (m)	1518	Cβ-asym rock (87)
1378 (m)	1378 (m)	1448	Cβ-sym rock (43); Cβ-sym bend (40)	1378 (s)	1378 (m)	1449	Cβ-sym rock (45); Cβ-sym bend (41)
1354 (s)	1354 (m)	1408	Nt−Cα−Hα (38); $CtOO^-$ sym st (12)	1340 (s)	1340 (m)	1399	$CtOO^-$-sym st (50); Cα−Ct (13)
		1397	$CtOO^-$ sym st (29); Cβ−Cα−H (20); Nt−Cα−Hα (12); Cα−Ct (8)			1391	Nt−Cα−Hα (48); Cβ−Cα−Hα (35)
1304 (m)	1303 (m)	1357	Hα−Cα−Ct (28); COO^- sym st (21); Cβ−Cα−Hα (17)	1293 (m)	1292 (w)	1346	Hα−Cα−Ct (38); Nt−Cα−Hα (16); COO^--sym st (11); Cβ−Cα−Hα (11)
						1267	NtD_3^+-asym bend (34); W (D−O−D) (33)
						1261	W(D−O−D) (51); NtD_3^+-asym bend (21); NtD_3^+-asym bend (9)
						1228	NtD_3^+-sym bend (27); NtD_3^+-sym rock (25); ND_3^+-asym bend (10); W···NtD_3^+ (8)
1217 (w)	1215 (w)	1259	NtH_3^+-asym rock (21); Cβ-asym bend (16); Cβ−Cα−Hα (8); Nt−Cα−Hα (8)				
1136 (sh)	1136 (sh)	1190	NtH_3^+-asym rock (45); Hα−Cα−Ct (23); NtH_3^+-asym rock (12)		1177 (w)	1191	NtD_3^+-asym bend (13); Cα−Cβ (12); Cβ-asym bend (12); NtD_3^+-sym rock (9); W···NtD_3^+ (9); NtD_3^+-sym bend (9)
					1150 (sh)	1168	NtD_3^+-asym bend (40); Cβ-asym bend (16)
1113 (m)	1113 (m)	1106	Cβ-asym bend (44); Cα−Cβ (15); Nt−Cα (9); Cβ−Cα−Ct (9)	1100 (m)	1098 (w)	1113	Cβ-asym bend (47); Hα−Cα−Ct (13); Cβ−Cα−Ct (8)
1075 (w)		1045	Cβ-asym bend (31); W···W (10)	1055 (m)		1065	Cα−Cβ (29); Nt−Cα−Ct (12); Cβ-asym bend (10); Hα−Cα−C (8); Nt−Cα (8)
1003 (m)		1020	Ct−Cβ (36); Cβ-asym bend (18)		1020 (w)		
923 (m)		923	W···O−Ct (16); Nt−Cα (10); Cα−C (9); W···W (9)	918 (m)	917 (w)	918	NtD_3^+-asym rock (29); Cβ-asym bend (23); Cα−Cβ (8)
		891	Nt−Cα (24); W···O−C (17); Cβ-asym bend (13); Cα−Ct (10)	874 (m)		894	Cβ-asym bend (23); Nt−Cα (20); Cα−Ct (15)
848 (s)		828	Nt−Cα (23); O−Ct−O (14); Cα−Ct−O sym bend (9); Cα−Ct (8)	833 (sh)		856	ND_3^+-asym rock (36); W···NtD_3^+ (16); Cα−Cβ (9)
				812 (m)		813	Nt−Cα (22); OCtO (17); Cα−Cβ (10); NtD_3^+-asym rock (9)
777 (w)		783	W···O−Ct (73); W5···W1 (13); Nt−Cα−Ct (9)	768 (w)		792	W···O−Ct (23); W···O−Ct (19); Nt−Cα (16)

[a] s, intense; m, medium; w, weak; sh, shoulder. Ct and Nt refer to the carbon and nitrogen atoms of the terminal COO^- and NH_3^+ groups, respectively. Raman: Vibrational wavenumbers in Raman spectra recorded in H_2O and D_2O buffers (Figure 2). IR: Vibrational wavenumbers observed in FT-IR ATR spectra recorded in H_2O and D_2O (Figure 2). Calcd: Calculated results obtained at the DFT/B3LYP/6-31++G* level on a theoretical model including alanine surrounded by five water molecules (Figure 6). Assignments are based on the potential energy distribution (PED). In front of each internal coordinate is reported the corresponding PED (in percent). Only major contributions (PED ≥ 8%) are reported in this table.

of redundancies among vibrational coordinates and assignment of wavenumbers on the basis of the PED (potential energy distribution) matrix elements as expressed in terms of a combination of local symmetry and internal coordinates.[25] No scaling factor was applied in order to improve the agreement between the calculated and observed wavenumbers. In our opinion, the comparison between observed data and raw calculated results allows us to account for the discrepancies arising from different origins such as the incompleteness of the theoretical level, or the neglect of anharmonic effects.

In particular, the assignment of the vibrational modes involving CH_3 and NH_3^+ groups is performed on the basis of their C_{3v} local symmetry (antisymmetric and symmetric stretchings and bendings), whereas, for CH_2 groups, C_{2v} coordinates (bending, scissoring, rocking, wagging) are used. The letter "t" designates the terminal backbone atoms (Ct or Nt), whereas "α, β, γ, and δ" refer to the carbon atoms located in the branched side chains of the considered AAs (Figure 1).

III. Results

Experimental. The observed vibrational spectra of the three BCAAs studied in this work (A, V, and I) are displayed in Figures 2−4. Each figure shows for a given amino acid the Raman and FT-IR spectra recorded in H_2O and D_2O. Full vibrational data collected from leucine are reported in the first manuscript of this series.[25] Thus, by comparing the vibrational spectra of leucine[25] and isoleucine (present work), the reader can appreciate the main differences caused by their side chains (Figure 1). In Tables 1−3 are listed the wavenumbers and relative intensities of the main observed bands and shoulders.

Theoretical. In order to account for the spatial distribution of water molecules around each amino acid, the stereoviews of optimized supermolecules are displayed in Figures 5 and 6. Table 4 shows the values of electronic (E_e) and vibrational energies ($E_v = {}^1/_2\Sigma h\nu$, where h is the Plank constant and ν the frequency of a vibrational mode) for each supermolecule. Table 5 displays the geometrical parameters (bond lengths, angles, dihedral angles) for BCAAs, as well as their H-bond lengths with surround-

TABLE 2: Assignment of the Valine (V) Vibrational Modes Observed in Aqueous Solutions[a]

valine				valine-deuterated			
Raman	IR	calcd	assignment (PED%)	Raman	IR	calcd	assignment (PED%)
	1633 (sh)	1762	NtH_3^+-asym bend (48); W5(H−O−H) (14)				
1620 (sh)		1670	NtH_3^+-asym bend (31); NtH_3^+-asym bend (14)				
1597 (m)	1597 (s)	1656	COO^--asym st (55); W(H−O−H) (13)	1612 (m)	1612 (s)	1680	$CtOO^-$-asym st (81); CαCtO asym bend (8);
	1521 (s)	1613	NtH_3^+-sym bend (35); NtH_3^+-sym rock (32)				
1474 (s)		1537	Cγ1-asym bend (61); Cγ2-asym bend (24)	1473 (s)	1472 (w)	1537	Cγ1-asym bend (62); Cγ2-asym bend (23)
	1468 (m)	1533	Cγ1-asym bend (51); Cγ2-asym bend (33)			1533	Cγ1-asym bend (52); Cγ2-asym bend (31)
1447 (s)		1518	Cγ2-asym bend (52); Cγ1-asym bend (27)	1448 (s)		1518	Cγ2-asym bend (61); Cγ1-asym bend (26)
		1511	Cγ2-asym bend (56); Cγ1-asym bend (26)			1511	Cγ2-asym bend (56); Cγ1-asym bend (25)
1412 (s)	1411 (s)	1460	Cγ1-sym bend (35); Cγ1-sym rock (31); Cγ2-sym bend (12); Cγ2-sym rock (11)	1411 (s)	1410 (m)	1460	Cγ1-sym bend (35); Cγ1-sym rock (31); Cγ2-sym bend (12); Cγ2-sym rock (10)
1398 (sh)	1398 (sh)	1436	Cα−Cβ−Hβ (18); Nt−Cα−Hα (16); COO^--sym st (16); Cα−Ct (9)	1398 (sh)	1398 (sh)	1434	Cγ2-sym bend (38); Cγ2-sym rock (34); Cγ1-sym bend (12); Cγ1-sym rock (11)
		1434	Cγ2-sym bend (37); Cγ2-sym rock (33); Cγ1-sym bend (13); Cγ1-sym rock (11)			1428	$CtOO^-$-sym st (23); Cα−Cβ−Hβ (22); Cα−Ct (10)
	1379 (w)	1416	Nt−Cα−Hα (31); Cβ−Cα−Hα (31)		1380 (w)	1411	Nt−Cα−Hα (42); Cβ−Cα−H (32)
1358 (s)	1358 (s)	1371	COO^--sym st (45); Hα−Cα−C (11); Nt−Cα−Hα (8)	1355 (s)	1355 (m)	1368	$CtOO^-$-sym st (40); Nt−Cα−Hα (13); Hα−Cα−Ct (11)
1334 (s)	1334 (m)	1349	Cδ2−Cγ−Hγ (22); Cγ2−Cβ−Hβ (22)	1333 (s)	1334 (w)	1345	Cδ2−Cγ−Hγ (23); Cγ2−Cβ−Hβ (23)
1325 (s)	1324 (sh)	1329	Hα−Cα−Ct (17); Cβ−Cα−H (10); Cα-Cβ (8); Cα−Cβ−Hβ (8)	1316 (s)	1316 (w)	1323	Hα−Cα−Ct (26); Cβ−Cα−Hα (11)
						1267	W(D−O−D) (42); NtD_3^+-asym bend (28)
						1258	W(D−O−D) (35); NtD_3^+-asym bend (31)
						1228	NtD_3^+-sym bend (19); NtD_3^+-sym rock (17)
1272 (m)	1267 (w)	1237	Cα−Cβ (11); NtH_3^+-asym rock (10); Cβ−Cγ1 (9); Cγ1-asym rock (8); Cγ2-asym rock (8)	1266 (m)	1262 (w)	1219	Cγ1-asym rock (14); NtD_3^+-sym bend (13); Cγ2-asym rock (12); NtD_3^+-sym rock (11); Cα−Cβ (8)
1193 (m)		1201	Cγ2-asym rock(21); Cγ1-asym rock (18); Cβ−Cγ2 (11); NtH_3^+-asym rock (9)	1188 (w)		1190	NtD_3^+-asym bend (23); $NtD_3^+\cdots$W (9); NtD_3^+-asym bend (8)
1136 (m)		1179	NtH_3^+-asym rock (40); Hα−Cα−Ct (21)		1177 (w)	1169	NtD_3^+-asym bend (20); Cγ2-asym rock (12); NtD_3^+-asym bend (8)
1125 (m)		1120	Cγ1-asym rock (24); Cα−Cβ−Hβ (16); Cγ2-asym rock (14)	1129 (m)		1125	Cγ1-asym rock (34); Hα−Cα−Ct (12); Cα−Cβ−Hβ (9); Cβ−Cγ1 (8)
1067 m)		1099	NtH_3^+-asym rock (17); Cβ−Cγ1 (17); Cβ−Cγ2 (15); Cγ1-asym rock (10); Cγ2-asym rock (9)				
				1027 (m)	1020 (w)	1032	Cγ2-asym rock (21); Cα−Cβ (17); Nt−Cα−Ct (14)
1025 (w)	1019 (m)	1007	Nt−Cα (28); Cα−Cβ (21); Cγ2-asym rock (8)				
997 (w)		978	Cγ1-asym rock (29); Cβ−Cγ2 (25); Cγ2-asym rock (18); Cβ−Cγ1 (10)	980 (sh)		984	Cβ−Cγ2 (28); Cβ−Cγ1 (14); Cγ1-asym rock (14)
						975	Cγ2-asym rock (31); Cγ1-asym rock (15)
965 (m)		947	Cγ2-asym rock (35); Cγ1-asym rock (33)	964 (m)		942	Cγ1-asym rock (36); Cγ2-asym rock (25)
946 (s)		960	Nt−Cα (19); Cα−Ct (14); Cγ2-asym rock (10)	949 (sh)		962	Cα−Ct (19); Nt−Cα (18); NtD_3^+-asym rock (15)
891 (s)		877	Cα−-Ct (17); Cβ−Cγ2 (9)	876 (m)		896	Cβ−Cγ1 (32); Cβ−Cγ2 (16); NtD_3^+-asym rock (11)
850 (m)		840	Ct═O$\cdots$W (57); $NtH_3^+\cdots$W (30)				
827 (s)		826	Ct═O$\cdots$W (29); Cβ−Cγ1 (20); Nt−Cα (8)	829 (m)	829 (w)	839	NtD_3^+-asym rock (22); OCtO (21); CαCtO sym bend (10)
776 (sh)		771	W$\cdots$W (32); Ct═O$\cdots$W (26); OCtO (13)	787 (m)		800	C═O$\cdots$W (30); NtD_3^+-asym rock (20); Nt−Cα (16); Cβ−Cα−Ct (12)
759 (m)		714	Nt−Cα−Ct (13); CαCtO asym bend (9); Ct═O$\cdots$W (9)	738 (s)		766	Cα−Cβ (23); OCtO (10); Cβ−Cγ1 (9); $NtD_3^+\cdots$W (8)

[a] s, intense; m, medium; w, weak; sh, shoulder. Ct and Nt refer to the carbon and nitrogen atoms of the terminal COO^- and NH_3^+ groups, respectively. Raman: Vibrational wavenumbers in Raman spectra recorded in H_2O and D_2O buffers (Figure 3). IR: Vibrational wavenumbers observed in FT-IR ATR spectra recorded in H_2O and D_2O (Figure 3). Calcd: Calculated results obtained at the DFT/B3LYP/6-31++G* level on a theoretical model including valine surrounded by five water molecules (Figure 6). Assignments are based on the potential energy distribution (PED). In front of each internal coordinate is reported the corresponding PED (in percent). Only major contributions (PED ≥ 8%) are reported in this table.

ing water molecules. Finally, Table 6 reports a comparison between a selection of calculated wavenumbers derived from the supermolecules containing leucine surrounded by 5 and 12 (see ref 25 for more details) water molecules, respectively.

IV. Discussion

Reliability of Supermolecular Models Containing Five Water Molecules. The geometrical parameters of L+5W are reported in Table 5. The comparison between the bond lengths and angles of leucine interacting with 5 (present work) and 12 (see ref 25 for details) water molecules allows us to conclude that the variation of hydration number leads to some little changes in the L backbone geometrical parameters. We can note especially the variations in the bond lengths and angles of the terminal NtH_3^+ and $CtOO^-$ groups. Because of its hydrophobic character, the geometrical data of the L side chain remain independent of hydration number. Table 6 shows the sensitivity of a selection of characteristic modes (νNH_3^+, δNH_3^+, and δCOO^-) to the H-bond patterns with water molecules. A wavenumber downshift is generally observed for the stretching vibrations, whereas angle bendings are upshifted upon increasing n_w. The n_w increase leads to an improvement of the calculated wavenumbers; i.e., they get closer to the observed wavenumbers, except δNH_3^+. However, the relative variation of calculated wavenumbers

TABLE 3: Assignment of the Isoleucine (I) Vibrational Modes Observed in Aqueous Solutions[a]

isoleucine				isoleucine-deuterated			
Raman	IR	calcd	assignment (PED%)	Raman	IR	calcd	assignment (PED%)
	1635 (sh)	1765	NtH_3^+-asym bend (57)				
	1618 (sh)	1684	NtH_3^+-asym bend (39); $NtH_3^+\cdots W$ (11)				
1596 (w)	1594 (s)	1653	$CtOO^-$-asym st (56); W(H−O−H) (15)	1611 (m)	1611 (s)	1679	$CtOO^-$-asym st (83)
	1519 (s)	1593	NtH_3^+-sym bend (35); NtH_3^+-sym rock (33)				
1463 (s)	1465 (m)	1538	Cγ1-asym rock (48); Cδ-asym bend (33)	1465 (s)	1465 (w)	1538	Cγ1-asym rock (48); Cδ-asym bend (33)
		1528	Cδ-asym bend (54); Cγ1-asym rock (17); Cβ-scissor (16)			1528	Cδ-asym bend (53); Cβ-scissor (17); Cγ1-asym rock (17)
1446 (s)		1520	Cγ1-asym rock (48); Cδ-asym bend (33); Cβ-scissor (8)	1447 (s)		1520	Cγ1-asym rock(48); Cδ-asym bend (32); Cβ-scissor (9)
		1519	Cδ-asym bend (39); Cγ1-asym rock (40)			1519	Cδ-asym bend (40); Cγ1-asym rock (39)
		1505	Cδ-scissor (60); Cγ1-asym rock (19); Cδ-asym bend (9)			1505	Cβ-scissor (60); Cγ1-asym rock (20); Cδ-asym bend (9)
1412 (s)	1410 (s)	1441	Cγ1-sym rock (39); Cγ1-sym bend (35); Cδ-sym bend (10); Cδ-sym rock (9)	1412 (s)	1410 (m)	1440	Cγ1-sym rock (39); Cγ1-symbend (35); Cδ-sym bend (10); Cδ-sym rock (9)
		1435	Cδ-sym bend (39); Cδ-sym rock (34); Cγ1-sym rock (8)			1435	Cδ-sym bend (39); Cδ-symrock (34); Cγ1-sym rock (8)
1392(sh)	1393 (sh)	1423	Nt−Cα−Hα (25); Cβ−Cα−Hα (18); COO^--sym st (8)	1393 (sh)	1393 (sh)	1419	Cα−Cβ−Hβ (20); Cβ−Cα−Hα (18); Nt−Cα−Hα (15); Cβ-rock (9); $CtOO^-$-sym st (9)
1367 (sh)	1365 (sh)	1401	COO^--sym st (16); Cβ-rock (13); Hβ−Cβ−Cγ1 (8)		1365 (sh)	1398	$CtOO^-$-sym st (47); Cα−Ct (11)
1350 (s)	1350 (s)	1392	COO^--sym st (29); Nt−Cα−Hα (11); Cβ−Cα−Hα (11); Cβ-rock (9)	1353 (s)		1392	Cβ-rock (20); Cβ-bend (15); Nt−Cα−Hα (13); Cβ−Cα−Hα (11)
1338 (s)	1338 (s)	1379	Hβ−Cβ−Cγ2 (30); Hβ−Cβ−Cγ1 (17); Cβ-wag (12)	1335 (s)	1336 (w)	1376	Hβ−Cβ−Cγ (41); Cβ-wag (22); Cβ-rock (10)
1310 (m)	1311 (w)	1367	Cβ-rock (16); Cβ-wag (11); Hα−Cα−Ct (10); Nt−Cα−Hα (9); COO^--sym st (8)	1300 (m)		1355	Nt−Cα−Hα (35); Hα−Cα−Ct (17); Cα−Cβ−Hβ (16)
1264 (w)	1264 (w)	1326	Cβ-wag (20); Cβ-bend (15); Hβ−Cβ−Cγ2 (15); Hα−Cα−Ct (8)	1259 (m)		1324	Cβ-wag (21); Cβ-bend (17); Hβ−Cβ−Cγ (16); Hα−Cα−Ct (8)
1255 (w)		1284	Cβ-bend (20); Hα−Cα−Ct (15); Hβ−Cβ−Cγ1 (14); Cδ-asym rock (11)				
						1267	W (D−O−D) (37); NtD_3^+-asym bend (33)
						1261	W (D−O−D) (45); NtD_3^+-asym bend (24); Ct═O···W4 (9)
						1225	NtD_3^+-sym bend (36); NtD_3^+-sym rock (19); $NtD_3^+\cdots W$ (12)
1190 (w)	1190 (w)	1233	NtH_3^+-asym rock (20); Cβ−Cα−Hα (10); Cγ1-asym bend (9)	1175 (w)	1178 (w)	1191	Cγ1-asym bend (18); NtD_3^+-sym bend (10); NtD_3^+-sym rock (9)
1173 (w)		1188	Cγ1-asym bend (21); Cβ-twist (18); Cγ1−Cβ−Cγ2 (9); Cδ-asym rock (8)			1185	Cγ1-asym bend (18); Cβ-twist (14); Cδ-asym rock (10)
1136 (m)		1178	NtH_3^+-asym rock (45); Hα−Cα−Ct (19)	1131 (w)		1176	NtD_3^+-asym bend (41); $NtD_3^+\cdots W$ (8); Cγ1-asym bend (8)
1116 (m)		1148	Cβ−Cγ1 (20); Cβ−Cγ2 (17); Cδ-asym rock (16);	1113 (w)		1149	Cβ−Cγ1 (18); Cδ-asym rock (17); Cβ−Cγ2 (16); Cβ-rock (8)
1071 (m)		1093	NtH_3^+-asym rock (19); W···W (9); Cγ1-asym bend (8)				
1037 (m)		1047	Cγ1−Cδ (49); Cδ-asym rock (8)	1045 (m)		1059	Cγ1−Cδ (47); Cβ−Cγ1 (8)
998 (m)		1019	Cδ-asym rock (20); Nt−Cα (15)	1028 (m)	1022 (w)	1017	Cγ1−Cδ (16); Cγ1-asym bend (14); Nt−Cα−Ct (11)
990 (m)		992	Cγ1-asym bend (33); Cδ-asym rock (18); Cβ-wag (10)	981 (m)		1014	Cδ-asym rock (24); Cβ−Cγ2 (12); Cγ1-asym bend (9); NtD_3^+-asym rock (8); Cα−Ct (8)
965 (w)		976	Nt−Cα (28); Cβ−Cγ2 (23); Cγ1−Cδ (10)			991	Cδ-asym rock (22); Cγ1-asym bend (16); NtD_3^+-asym rock (8); Hβ−Cβ−Cγ1 (8)
924 (w)		948	Cα−Ct (14); Cγ1-asym bend (12)	950 (m)		967	Nt−Cα (30); Cβ−Cγ2 (21); Cα−Ct (8)
884 (m)		863	Nt−Cα (13); W···W (24); Ct═O···W (13); Cγ1-asym bend (12)	929 (m)		945	Cγ1-asym bend (34); NtD_3^+-asym rock (22)
819 (m)		854	Cβ−Cγ1 (20)	869 (m)		873	Cβ−Cγ1 (27); Cγ1-asym bend (9); Cγ1−Cδ (8); NtD_3^+-asym rock (8)
				832 (m)		843	OCtO (24); NtD_3^+-asym rock (22); CαCtO sym bend (9)
				795 (w)		816	Nt-Cα (19); NtD_3^+-asym rock (15); W···W (11)
763 (m)		768	Cβ-twist (16); Ct═O···W4 (9); Cδ-asym rock (9); Nt−Cα−Ct (8); Cβ−Cγ2 (8); W···O−Ct (8)	748 (s)		768	W···W (43); Cβ-twist (14); Ct═O···W (11); Cβ−Cγ (9)

[a] s, intense; m, medium; w, weak; sh, shoulder. Ct and Nt refer to the carbon and nitrogen atoms of the terminal COO^- and NH_3^+ groups, respectively. Raman: Vibrational wavenumbers in Raman spectra recorded in H_2O and D_2O buffers (Figure 3). IR: Vibrational wavenumbers observed in FT-IR ATR spectra recorded in H_2O and D_2O (Figure 3). Calcd: Calculated results obtained at the DFT/B3LYP/6-31++G* level on a theoretical model including isoleucine surrounded by five water molecules (Figure 6). Assignments are based on the potential energy distribution (PED). In front of each internal coordinate is reported the corresponding PED (in percent). Only major contributions (PED ≥ 8%) are reported in this table.

(stretching or bending) does not exceed 2% in going from $n_w = 5$ to $n_w = 12$. This is well below the difference between observed and calculated wavenumbers.

Influence of the Side Chain on the Geometrical Parameters and H-Bond Lengths. One of the main conclusions from these calculations is that the H-bond lengths between water

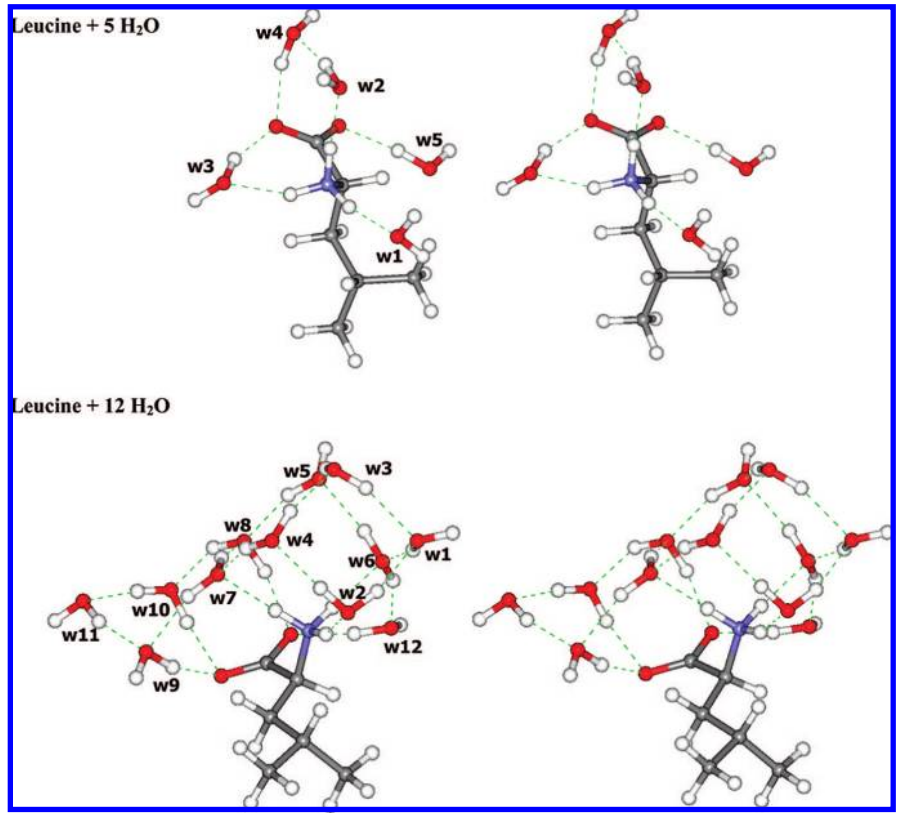

Figure 5. Stereoviews of the geometry optimized supermolecules composed of each leucine (L) and a number of water (W) molecules. L+5W (top, present work), L+12W (bottom, as taken from ref 25). Optimization at the DFT/B3LYP/6-31++G* level of theory. Note that five water molecules are necessary in order both to maintain the zwitterionic character and to hydrate satisfactorily the terminal groups of a BCAA.

TABLE 4: Electronic and Vibrational Energies of BCAAs Interacting with Five Surrounding Water Molecules[a]

	A+5W	V+5W	I+5W	L+5W
E_e	−705.961713	−787.585973	−823.903213	−823.892970
E_v	149.013	184.578	202.198	200.104

[a] A, alanine; V, valine; I, isoleucine; L, leucine; W, water molecule. E_e, electronic energy (Hartree); E_v, zero-point vibrational energy (kcal/mol).

molecules and terminal NtH_3^+ (or $CtOO^-$) groups show a general trend toward contraction when the size of the BCAA side chain increases, i.e., in going from A to L (Table 5).

Assignment of Observed Vibrational Data. ***1750−1500 cm^{-1} Spectral Region.*** Thanks to the existence of intense IR bands, the vibrational modes arising from NtH_3^+ angular bending and $CtOO^-$ out-of-phase stretching motions can be appreciated (Tables 1−3). NtH_3^+ bending modes observed at ca. 1640 and 1520 cm^{-1} in the IR spectrum disappear completely upon H/D isotopic substitution. Moreover, the calculations show that the NtH_3^+ bending modes are considerably coupled with those of surrounding water molecules through W···AA hydrogen bonds. On the other hand, the $CtOO^-$ asymmetric stretching mode at ca. 1600 cm^{-1} in H_2O is upshifted in D_2O, giving rise to intense and narrow IR bands located at ca. 1610 cm^{-1} (Figures 2−4).

1500−1200 cm^{-1} Spectral Region. Intense bands are conserved in Raman and IR spectra. $CtOO^-$ in-phase stretches and NH_3^+ angular bending take part in numerous vibrational modes in this region. Useful information on the side chain vibrational modes (CH_2 and CH_3 groups) can also be obtained. The number of observed bands increases with the size of the AA side chain.

Below 1200 cm^{-1}. Raman spectra present a wealth of information in this spectral region. The observed bands arise from both the backbone and side chain of the AAs. Alanine with its simple side chain gives rise to a limited number of intense and resolved bands; the most intense one at 848 cm^{-1} (Figure 2) is mainly assigned to the backbone vibrational motions involving the C_α atom. Vibrational modes are sensitive to deuteration because of their coupling with the $N_tH_3^+$ group motions. The assignment of the vibrational modes clearly evidences the coupling of water molecules with the backbone of different AAs, below 1000 cm^{-1}.

V. Concluding Remarks

In this report, we attempted to assign the vibrational data obtained from the aqueous samples of three AAs with hydrophobic side chains containing nonlabile hydrogens. H/D isotopic shifts of the vibrational bands observed in heavy water were considered in our interpretation. We have shown that quantum mechanical calculations at the DFT/B3LYP/6-31++G* level of theory, performed on a cluster containing five water molecules interacting with the backbone of each amino acid, permit an optimal assignment of observed vibrational data.

TABLE 5: Prominent Geometrical Parameters Derived from the Geometry Optimized Alanine (A), Valine (V), Isoleucine (I), and Leucine (L) Surrounded with Five Water (W) Molecules[a]

bond length	A+5W	V+5W	I+5W	L+5W	angle	A+5W	V+5W	I+5W	L+5W
Nt−H(1)	1.041	1.041	1.043	1.048	H(1)−Nt−H(2)	106.16	106.09	106.20	107.10
Nt−H(2)	1.029	1.027	1.030	1.031	H(1)−Nt−H(3)	106.37	105.39	105.84	106.60
Nt−H(3)	1.040	1.039	1.035	1.038	H(2)−Nt−H(3)	113.36	112.97	113.14	110.07
Nt−Cα	1.523	1.521	1.524	1.511	H(1)−Nt−Cα	110.72	109.42	109.76	111.37
Cα−Hα	1.089	1.088	1.090	1.092	H(2)−Nt−Cα	109.38	109.52	110.59	110.51
Cα−Ct	1.552	1.553	1.553	1.555	H(3)−Nt−Cα	110.73	113.09	111.12	111.01
Ct−O1	1.276	1.277	1.276	1.275	Cα−Ct−O1	116.11	116.71	116.15	116.87
Ct−O2	1.247	1.247	1.248	1.245	Cα−Ct−O2	116.83	116.38	116.94	116.24
					O1−Ct−O2	126.92	126.77	126.79	126.87
Cα−C*β*	1.525	1.544	1.540	1.536	Nt−Cα−C*β*	110.44	112.38	111.81	111.25
C*β*−H*β*		1.103	1.098		Nt−Cα−Hα	105.27	104.08	105.24	106.30
C*β*−H*β*(1)	1.095			1.099	Nt−Cα−Ct	106.99	107.09	106.36	109.62
C*β*−H*β*(2)	1.097			1.097	Ct −Cα− Hα	108.53	107.45	108.51	107.80
C*β*−H*β*(3)	1.093				C*β*−Cα−Hα	110.25	107.39	109.78	110.56
C*β*−C*γ*				1.545	Ct−Cα−C*β*	114.87	117.52	114.64	111.13
C*β*−C*γ*1		1.537	1.545		Cα−C*β*−H*β*		105.66	107.64	
C*β*−C*γ*2		1.540	1.540		Cα−C*β*−H*β*(1)	108.86			108.35
C*γ*−H*γ*				1.102	Cα−C*β*−H*β*(2)	110.95			106.35
C*γ*1−H*γ*1(1)		1.096			Cα−C*β*−H*β*(3)	111.82			
C*γ*1−H*γ*1(2)		1.095			H*β*(1)−C*β*−H*β*(2)	107.76			106.74
C*γ*1−H*γ*1(3)		1.094			H*β*(1)−C*β*−H*β*(3)	108.36			
C*γ*2−H*γ*2(1)		1.096	1.098		H*β*(2)−C*β*−H*β*(3)	108.97			
C*γ*2−H*γ*2(2)		1.096	1.095		Cα−C*β*−C*γ*				116.91
C*γ*2−H*γ*2(3)		1.096	1.094		Cα−C*β*−C*γ*1		115.99	111.59	
C*γ*−C*δ*1				1.538	Cα−C*β*−C*γ*2		108.63	108.72	
C*γ*−C*δ*2				1.538	C*γ*−C*β*−H*β* (1)				109.26
C*γ*1−C*δ*			1.535		C*γ*−C*β*−H*β* (2)				108.74
C*δ*−H*δ*(1)			1.098		C*γ*1−C*β*−C*γ*2		110.67		
C*δ*−H*δ*(2)			1.096		C*γ*1−C*β*−H*β*		108.10		
C*δ*−H*δ*(3)			1.095		C*γ*2−C*β*−H*β*		107.35		
C*δ*1−H*δ*1(1)				1.098	C*β*−C*γ*−H*γ*				108.82
C*δ*1−H*δ*1(2)				1.096	C*β*−C*γ*−C*δ*1				112.49
C*δ*1−H*δ*1(3)				1.097	C*β*−C*γ*−C*δ*2				109.43
C*δ*2−H*δ*2(1)				1.097	C*δ*1−C*γ*−C*δ*2				110.43
C*δ*2−H*δ*2(2)				1.097	C*δ*1−C*γ*−H*γ*				108.58
C*δ*2−H*δ*2(3)				1.098	C*δ*2−C*γ*−H*γ*				106.92
					C*β*−C*γ*1−H*γ*1(1)		109.14	109.70	
					C*β*−C*γ*1−H*γ*1(2)		111.24	109.12	
					C*β*−C*γ*1−H*γ*1(3)		113.30		
					C*β*−C*γ*1−C*δ*			114.34	

H-bond	A+5W	V+5W	I+5W	L+5W	angle	A+5W	V+5W	I+5W	L+5W
(W)O···H(Nt)	1.854	1.864	1.872	1.785	C*δ*−C*γ*1−H*γ*1(1)			107.57	
(W)O···H(Nt)	1.888	1.909	1.879	1.844	C*δ*−C*γ*1−H*γ*1(2)			109.67	
(W)O···H(Nt)	2.022	2.137	1.972	1.920	H*γ*1(1)−C*γ*1−H*γ*1(2)		108.08	106.12	
					H*γ*1(1)−C*γ*1−H*γ*1(3)		107.40		
(W)H···O(Ct)	1.751	1.737	1.757	1.751	H*γ*1(2)−C*γ*1−H*γ*1(3)		107.48		
(W)H···O(Ct)	1.753	1.768	1.763	1.759	C*β*−C*γ*2−H*γ*2(1)		110.02	111.08	
(W)H···O(Ct)	1.951	1.997	1.938	1.791	C*β*−C*γ*2−H*γ*2(2)		111.11	111.48	
					C*β*−C*γ*2−H*γ*2(3)		111.76	110.87	
					H*γ*2(1)−C*γ*2−H*γ*2(2)		107.97	107.82	
					H*γ*2(1)−C*γ*2−H*γ*2(3)		108.11	107.97	
					H*γ*2(2)−C*γ*2−H*γ*2(3)		107.73	107.45	
					C*γ*1−C*δ*−H*δ*(1)			111.12	
					C*γ*1−C*δ*−H*δ*(2)			110.54	
					C*γ*1−C*δ*−H*δ*(3)			112.12	
					H*δ*(1)−C*δ*−H*γ*2(2)			107.64	
					H*δ*(1)−C*δ*−H*γ*2(3)			107.83	
					H*δ*(2)−C*δ*−H*γ*2(3)			107.39	
					C*γ*−C*δ*1−H*δ*1(1)				110.54
					C*γ*−C*δ*1−H*δ*1(2)				110.93
					C*γ*−C*δ*1−H*δ*1(3)				112.74
					H*δ*1(1)−C*δ*1−H*δ*1(2)				108.14
					H*δ*1(1)−C*δ*1−H*δ*1(3)				108.78
					H*δ*1(2)−C*δ*1−H*δ*1(3)				106.09
					C*γ*−C*δ*2−H*δ*2(1)				111.08
					C*γ*−C*δ*2−H*δ*2(2)				111.48
					C*γ*−C*δ*2−H*δ*2(3)				110.76
					H*δ*1(1)−C*δ*2−H*δ*2(2)				107.83
					H*δ*1(1)−C*δ*2−H*δ*2(3)				107.72
					H*δ*1(2)−C*δ*2−H*δ*2(3)				107.81

[a] For atom numbering and chemical structures, see Figure 1. Optimized geometries are displayed in Figures 5 and 6. Ct and Nt refer to the carbon and nitrogen atoms of the terminal COO^- and NH_3^+ groups, respectively. Bond lengths are in angstroms and angles in degrees. H-bond distances (Å) between the hydrogen atoms of water (W) molecules and the terminal $CtOO^-$ group, and between the oxygen atoms of the water molecules and the terminal NH_3^+ group, are sorted in an increasing order in order to show their evolution from one amino acid to another.

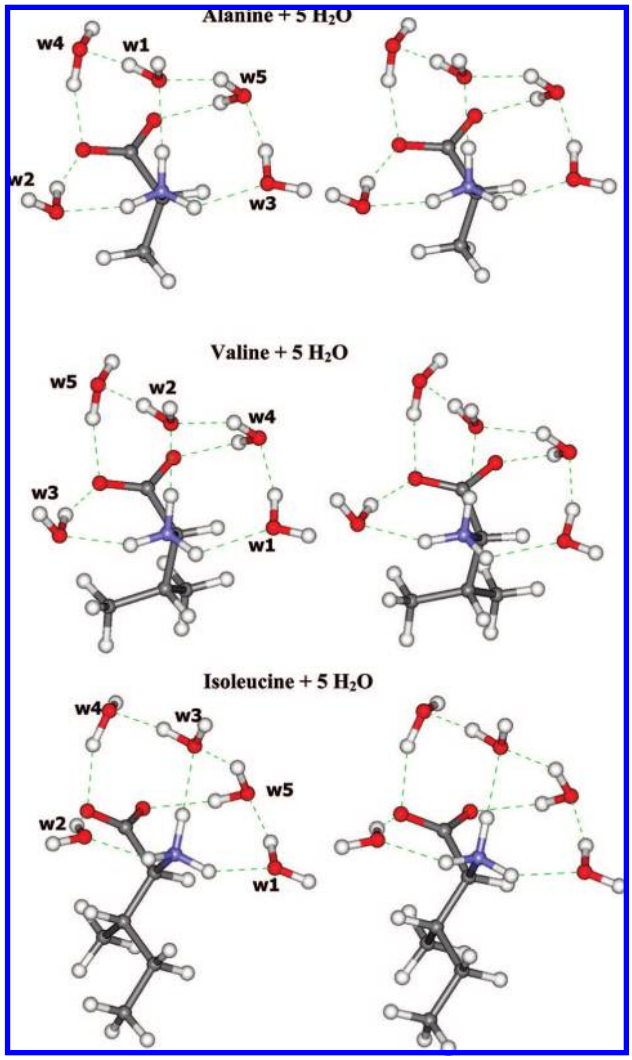

Figure 6. Stereoviews of the geometry optimized supermolecules composed of a BCAA and five water molecules forming H-bonds with each other and the two extreme polar heads (NH_3^+ and COO^-). From top to bottom: A+5W, V+5W, I+5W. Optimization at the DFT/B3LYP/6-31++G* level of theory.

TABLE 6: Selection of the Leucine Vibrational Modes Arising from the Bond-Stretch and Angular Bending Motions of the Backbone Terminal NH_3^+ and COO^- Groups[a]

observed		calculated		
R	IR	L+5W	L+12W	
		3364[b]	3215[b]	
		3226[b]	3096[b]	$\nu(NtH_3^+)$
		3070[c]	3003[c]	
	1644	1771[b]	1785[b]	
	1535	1750[b]	1771[b]	$\delta(NtH_3^+)$
	1514	1669[c]	1652[c]	
1600	1594	1669[b]	1643[b]	$\nu(CtOO^-)$
1414	1410	1384[c]	1417[c]	

[a] R, Raman; IR, ATR FT-IR, depicted vibrational data reported previously for leucine in hydrated media.[25] L+5W: Calculated at the DFT/B3LYP/6-31++G* level (present work). L+12W: Calculated at the DFT/B3LYP/6-31++G* level on a cluster containing leucine and 12 water molecules.[25] The letter t refers to the terminal nitrogen and carbon atoms of the leucine backbone. [b] Asymmetric vibrational motions. [c] Symmetric vibrational motions.

Acknowledgment. The authors would like to thank the *Agence Universitaire de la Francophonie* (AUF) for the financial support to the scientific project (ref 6313PS567). M.N. acknowledges AUF for a postdoctoral fellowship. We would also like to thank two French supercomputer centers: IDRIS (Orsay, France) and CINES (Montpellier, France) for the computational facilities on IBM workstation networks.

Supporting Information Available: Atomic Cartesian coordinates of the optimized geometries. This material is available free of charge via the Internet at http://pubs.acs.org.

References and Notes

(1) Schulz, G. E.; Schrimer, R. H. In *Principles of Protein Structure*; Cantor, R. H., Ed.; Springer-Verlag: New York, 1990.
(2) *Protein-lipid interactions*; Tamm, L. K., Ed. Wiley-VCH: 2005.
(3) Baumruk, V.; Huo, D.; Dukor, R. K.; Keiderling, T. A.; Lelievre, D.; Brack, A. *Biopolymers* **1994**, *34*, 1115–1121.
(4) Morris, M. C.; Vidal, P.; Chaloin, L.; Heitz, F.; Divita, G. *Nucleic Acids Res.* **1997**, *25*, 2730–2736.
(5) Castano, S.; Desbat, B.; Laguerre, M.; Dufourcq, J. *Biochim. Biophys. Acta* **1999**, *1416*, 176–194.
(6) Taylor, S. E.; Desbat, B.; Blaudez, D.; Jacobi, S.; Chi, L. F.; Fuchs, H.; Schwarz, G. *Biophys. Chem.* **2000**, *87*, 63–72.
(7) Castano, S.; Desbat, B.; Dufourcq, J. *Biochim. Biophys. Acta* **2000**, *1463*, 65–80.
(8) Avrahami, D.; Oren, Z.; Shai, Y. *Biochemistry* **2001**, *40*, 12591–12603.
(9) Li, W.; Nicol, F.; Francis, C., Jr. *Adv. Drug Delivery Rev.* **2004**, *56*, 967–985.
(10) Lamazière, A.; Chassaing, G.; Trugnan, G.; Ayala-Sanmartin, J. *J. Soc. Biol.* **2006**, *200*, 229–233.
(11) Hernandez, B.; Boukhalfa-Heniche, F. Z.; Seksek, O.; Coïc, Y. M.; Ghomi, M. *Biopolymers* **2006**, *81*, 8–19.
(12) Guiffo-Soh, G.; Hernandez, B.; Coïc, Y. M.; Boukhalfa-Heniche, F. Z.; Ghomi, M. *J. Phys. Chem. B* **2007**, *111*, 12563–12572.
(13) Guiffo-Soh, G.; Hernandez, B.; Coïc, Y. M.; Boukhalfa-Heniche, F. Z.; Fadda, G.; Ghomi, M. *J. Phys. Chem. B* **2008**, *112*, 1282–1289.
(14) Lins, L.; Decaffmeyer, M.; Thomas, A.; Brasseur, R. *Biochim. Biophys. Acta* **2008**, *1778*, 1537–1544.
(15) Karlsson, H. K.; Nilsson, P. A.; Nilsson, J.; Chibalin, A. V.; Zierath, J. R.; Blomstrand, E. *Am. J. Physiol. Endocrinol. Metab.* **2004**, *287*, E1–7.
(16) Blomstrand, E.; Eliasson, J.; Karlsson, H. K.; Köhnke, R. *J. Nutr.* **2006**, *136*, 269S–273S.
(17) Wolpert, M.; Hellwig, P. *Spectrochim. Acta, Part A* **2006**, *64*, 987–1001.
(18) Overman, S. A., Jr. *Biochemistry* **1999**, *38*, 4018–4027.
(19) Császár, A. G. *J. Mol. Struct.* **1995**, *346*, 141–152.
(20) Stepanian, S. G.; Reva, I. D.; Radchenko, E. D.; Adamowicz, L. *J. Phys. Chem. A* **1998**, *102*, 4623–4629.
(21) Frimand, K.; Bohr, H.; Jalkanen, K. J.; Suhai, S. *Chem. Phys.* **2000**, *255*, 165–194.
(22) Kumar, S.; Kumar Rai, A.; Rai, S. B.; Rai, D. K.; Singh, V. B. *J. Mol. Struct.* **2006**, *791*, 23–29.
(23) Stepanian, S. G.; Reva, I. D.; Radchenko, E. D.; Adamowicz, L. *J. Phys. Chem. A* **1999**, *103*, 4404–4412.
(24) Lima, J. A., Jr.; Freire, P. T. C.; Lima, R. J. C.; Moreno, A. J. D.; Mendes Filho, J.; Melo, F. E. A. *J. Raman Spectrosc.* **2005**, *36*, 1076–1081.
(25) Derbel, N.; Hernandez, B.; Pflüger, F.; Liquier, J.; Geinguenaud, F.; Jaïdane, N.; Ben Lakhdar, Z.; Ghomi, M. *J. Phys. Chem. B* **2007**, *111*, 1470–1477.
(26) Wang, W.; Pu, X.; Zheng, W.; Wong, N. B.; Tian, A. *THEOCHEM* **2003**, *626*, 235–244.
(27) Ramaekers, J.; Pajak, J.; Lambie, B.; Maes, G. *J. Chem. Phys.* **2004**, *120*, 4182–4193.
(28) Balta, B.; Aviyente, V. *J. Comput. Chem.* **2003**, *24*, 1789–1802.
(29) Balta, B.; Aviyente, V. *J. Comput. Chem.* **2004**, *25*, 690–703.
(30) Leung, K.; Rempe, S. B. *J. Chem. Phys.* **2005**, *122*, 18405–18418.
(31) Becke, A. D. *J. Chem. Phys.* **1993**, *98*, 5648–5652.
(32) Lee, C.; Yang, W.; Parr, R. G. *Phys. Rev. B* **1988**, *37*, 785–789.
(33) Frisch, M. J.; Trucks, G. W.; Schlegel, H. B.; Scuseria, G. E.; Robb, M. A.; Cheeseman, J. R.; Montgomery, J. A., Jr.; Vreven, T.; Kudin, K. N.; Burant, J. C.; Millam, J. M.; Iyengar, S. S.; Tomasi, J.; Barone, V.; Mennucci, B.; Cossi, M.; Scalmani, G.; Rega, N.; Petersson, G. A.; Nakatsuji, H.; Hada, M.; Ehara, M.; Toyota, K.; Fukuda, R.; Hasegawa, J.; Ishida, M.; Nakajima, T.; Honda, Y.; Kitao, O.; Nakai, H.; Klene, M.; Li, X.; Knox, J. E.; Hratchian, H. P.; Cross, J. B.; Bakken, V.; Adamo, C.;

Jaramillo, J.; Gomperts, R. ; Stratmann, R. E.; Yazyev, O.; Austin, A. J.; Cammi, R.; Pomelli, C.; Ochterski, J. W.; Ayala, P. Y.; Morokuma, K.; Voth, G. A.; Salvador, P.; Dannenberg, J. J.; Zakrzewski, V. G.; Dapprich, S.; Daniels, A. D.; Strain, M. C.; Farkas, O.; Malick, D. K.; Rabuck, A. D.; Raghavachari, K.; Foresman, J. B.; Ortiz, J. V.; Cui, Q.; Baboul, A. G.; Clifford, S.; Cioslowski, J.; Stefanov, B. B.; Liu, G.; Liashenko, A.; Piskorz, P.; Komaromi, I.; Martin, R. L.; Fox, D. J.; Keith, T.; Al-Laham, M. A.; Peng, C. Y.; Nanayakkara, A.; Challacombe, M.; Gill, P. M. W.; Johnson, B.; Chen, W.; Wong, M. W.; Gonzalez, C.; Pople, J. A. *Gaussian 03*, revision C.02; Gaussian, Inc.: Wallingford, CT, 2004.

(34) Gaigeot, M. P.; Ghomi, M. *J. Phys. Chem. B* **2001**, *105*, 5007–5017.

JP809204D